Dual-Band Filtering Differential Phase Shifter Using Cascaded Wideband Phase Shifter and Bandstop Network With Two Same Phase Shifts

Lei-Lei Qiu, *Graduate Student Member, IEEE*, and Lei Zhu, *Fellow, IEEE*

***Abstract*— This letter proposes a new design method of dual-band filtering differential phase shifter using cascaded wideband phase shifter and bandstop network. After cascading the bandstop network, the phase shift characteristic of the initial wideband filtering differential phase shifter remains unchanged, while its wide passband is divided into dual subpassbands. Compared with traditional dual-band-filter-based topology, the proposed cascaded one features the advantage of independently controlled phase and amplitude responses, and can achieve the same phase shifts in two passbands that conventional one cannot. For verification, a dual-band differential phase shifter with two same phase shifts of 90° is designed, fabricated, and measured. Simulated and measured results show good agreement.**

***Index Terms*— Bandstop network, differential phase shifter, dual-band, filtering, wideband phase shifter.**

I. Introduction

DIFFERENTIAL phase shifters have been widely used in beamforming networks, phased array antenna systems, etc., and have been extensively investigated so far [1]–[7]. Recently, as the rapidly rising trend of multifunctional and highly integrated devices, various high-performance differential phase shifters with filtering response have attracted great attention [8]–[15]. However, the research of dual-band filtering phase shifters, which are desirable for dual-band point-to-multipoint multitask communication, sensing, and radar applications, is relatively deficient. In [11], two sets of different loaded-lines were utilized to switch the phase states at two frequencies, while it failed to achieve concurrent dual-band operation at the same time. In [12] and [13], two different dual-frequency phase shifters were proposed, respectively, while they are primarily designed at two individual frequency points. To achieve predetermined phase shift values in two bands, the coupled resonator type was developed [14]. However, this structure holds the theoretical limit of $\Delta\varphi_2/\Delta\varphi_1 \geq f_2/f_1$. In [15], a branch line structure was adopted for dual-band phase shifter, while the bandwidths cannot be controlled independently. In addition, it can be inferred that the dual-band phase shifter also has the limitation of $\Delta\varphi_2/\Delta\varphi_1 \geq f_2/f_1$, which greatly limits its application scenarios, such as potential dual-feed structure with required $\Delta\varphi_2 = \Delta\varphi_1 = \pm 90°$ for dual-band circularly polarized (CP) antennas with same polarized rotations.

To address the above-mentioned issues, dual-band filtering differential phase shifter is proposed using cascaded wideband filtering phase shifter and bandstop network. Different from traditional dual-band phase shifters, the proposed one breaks through the limitation of $\Delta\varphi_2/\Delta\varphi_1 \geq f_2/f_1$, and can achieve the same phase shifts in the two passbands, i.e., $\Delta\varphi_2 = \Delta\varphi_1$. Moreover, a few advanced performances, such as the flexible realization of frequency ratio, absolute bandwidths, and wide stopband, can be obtained as expected.

II. Working Principle

Fig. 1 depicts the generalized topology of the conventional wideband differential phase shifter and the proposed dual-band type. To be more versatile, the two paths of the conventional type are represented by transmission lines with equivalent characteristic impedance Z_0 and electrical lengths of θ_r and θ_m, where θ_r and θ_m are functions of θ_0, $\theta_0 = 0.5\,\pi f/f_0$, and f_0 is the center frequency of the working passband. As for the proposed type, two same networks, which have an equivalent characteristic impedance of Z_c and electrical length of θ_c, are individually cascaded after the two paths of the traditional type, where θ_c is also a function of θ_0. As for the conventional type, the ABCD matrix of the reference (main) math is

$$\begin{bmatrix} A_i & B_i \\ C_i & D_i \end{bmatrix} = \begin{bmatrix} \cos\theta_i & jZ_0\sin\theta_i \\ j\sin\theta_i/Z_0 & \cos\theta_i \end{bmatrix}. \tag{1}$$

Then, the amplitude and phase responses of the two paths can be calculated as

$$\varphi_i = \tan^{-1}[(-B_i - C_i Z_0 Z_L)/j(A_i Z_L + D_i Z_0)] \tag{2-a}$$

$$|T_i| = 2\sqrt{Z_0 Z_L}/\sqrt{(A_i Z_L + D_i Z_0)^2 - (B_i + C_i Z_0 Z_L)^2} \tag{2-b}$$

where $\varphi_{(i)}$ and $T_{(i)}$ are the phase characteristic and the transmission coefficient, $i = r$ or m corresponds to the reference or main path. Furthermore, they can be simplified as

$$\tan(\varphi_m - \varphi_r) = \frac{\tan\varphi_m - \tan\varphi_r}{1 + \tan\varphi_m \tan\varphi_r} = \frac{\sin\theta_r\cos\theta_r - \sin\theta_m\cos\theta_m}{\cos^2\theta_r - \sin^2\theta_m} \tag{3-a}$$

$$|T_r| = |T_m| = 2\sqrt{Z_0 Z_L}/(Z_L + Z_0). \tag{3-b}$$

Manuscript received October 22, 2020; revised December 1, 2020; accepted December 18, 2020. Date of publication January 4, 2021; date of current version March 11, 2021. This work was supported in part by the Macao Science and Technology Development Fund under the Science and Technology Development Fund (FDCT). Research Grant 0095/2019/A2, in part by the National Natural Science Foundation of China under General Program 61971475, and in part by the University of Macau through Multiyear Research under Grant MYRG2017-00007-FST and Grant MYRG2018-00073-FST. *(Corresponding author: Lei Zhu.)*

The authors are with the Department of Electrical and Computer Engineering, Faculty of Science and Technology, University of Macau, Zhuhai 999078, Macau SAR China (e-mail: yb87440@connect.um.edu.mo; leizhu@umac.mo).

Color versions of one or more figures in this letter are available at https://doi.org/10.1109/LMWC.2020.3046247.

Digital Object Identifier 10.1109/LMWC.2020.3046247

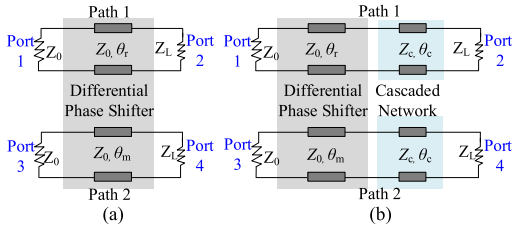

Fig. 1. Topology of the differential phase shifter. (a) Conventional wideband type. (b) Proposed dualband type.

As for the proposed type, the ABCD matrices of the reference path and main path are

$$\begin{bmatrix} A_i & B_i \\ C_i & D_i \end{bmatrix} = \begin{bmatrix} \cos\theta_i & jZ_0\sin\theta_i \\ j\sin\theta_i/Z_0 & \cos\theta_i \end{bmatrix} \begin{bmatrix} \cos\theta_c & jZ_c\sin\theta_c \\ j\sin\theta_c/Z_c & \cos\theta_c \end{bmatrix}. \tag{4}$$

Similarly, the phase shift and amplitude of the proposed type are deduced as

$$\tan(\varphi_m - \varphi_r) = \frac{\sin\theta_r\cos\theta_r - \sin\theta_m\cos\theta_m}{\cos^2\theta_r - \sin^2\theta_m} \tag{5-a}$$

$$|T_r| = |T_m| = \frac{2Z_c\sqrt{Z_0Z_L}}{\sqrt{\left(Z_c^2+Z_0Z_L\right)^2 - \left(Z_c^2-Z_0^2\right)\left(Z_c^2-Z_L^2\right)\cos^2\theta_c}}. \tag{5-b}$$

Obviously, from (3) and (5), after cascading the same network, the amplitude characteristic of the differential phase shifter is changed accordingly, while its phase shift response keeps constant. Therefore, the desired amplitude characteristic but almost the same phase characteristic can be readily realized. In other words, the phase and amplitude responses can be controlled independently. It should be further pointed out that the form of the cascade network is not limited, and it can be a bandstop network, low-pass network, and an impedance transformation network for different scenarios.

This letter aims at the design of dual-band filtering differential phase shifter through cascading a bandstop network. The design concept is demonstrated in Fig. 2. Through the same cascaded bandstop networks, the phase-shifting passband $(\theta_1 - \theta_2)$ of the phase shifter is suppressed by the stopband $(\theta_3 - \theta_4)$, such that two desired passbands with the same phase shifts are constructed. Since the phase shift and amplitude characteristics are relatively independent, the design procedure of the proposed differential phase shifter is simplified to separately design the wideband phase shifter and the bandstop network, and then cascade them together.

III. Dual-Band Filtering Differential Phase Shifter

To demonstrate the above method, Fig. 2 depicts the specific circuit diagram of the proposed differential phase shifter, where the two paths of the wideband phase shifter adopt the differential-mode structure proposed in [16], which is composed of coupled multimode resonators to achieve a wideband filtering phase shift. The bandstop network adopts a branch line structure [17], [18]. The impedance and electrical length of the middle connecting line are Z_c and θ_c, and those of the shunted short-circuited stub are Z_d and 2 θ_c, respectively.

Fig. 3 plots the responses of the phase shifter under different stopband bandwidths, where the parameters of the wideband

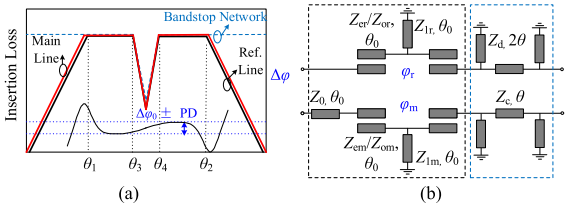

Fig. 2. Working principle and circuit model of the proposed differential phase shifter. (a) Working principle. (b) Circuit model.

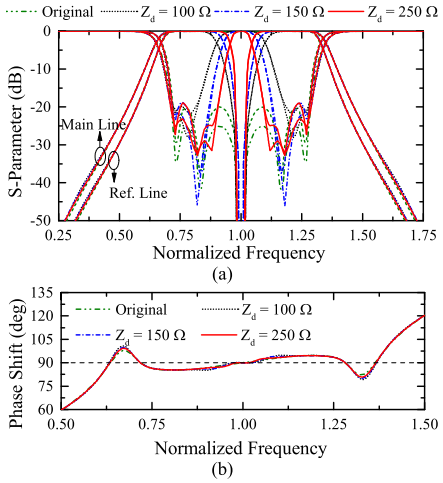

Fig. 3. Simulated responses of the proposed phase shifter under different Z_d of the bandstop network ($Z_c = 50\ \Omega$). (a) Amplitude. (b) Phase shift.

phase shifter are $\theta_1 = 65°$, $\theta_2 = 115°$, $\Delta\varphi_0 = 90°$, $PD = 5°$, $f_0 = 2$ GHz. The bandstop network has the same center frequency as the phase shifter, that is, $\theta_c = \theta_0 = 0.5\ \pi\ @\ f_0$. It can be seen that before the cascading bandstop network, the wideband phase shifter can achieve a 61% wideband phase shift within $90° \pm 4.6°$. After cascading the bandstop network, the proposed phase shifter realizes dual filtering passbands in amplitude. When impedance Z_d of the short-circuited stub gradually increases, the stopband bandwidth gradually decreases to a notch, while the bandwidths of the two passbands increase accordingly. As a result, the center frequency ratio f_2/f_1 of these two passbands is decreased, although the absolute bandwidth ratio keeps constant. Theoretically, under the extreme case of $\theta_3 = \theta_1$ and $\theta_4 = \theta_2$, the center frequency ratio of the two passbands becomes the largest, which is equal to $f_2/f_1 = \theta_2/\theta_1$. Considering an achievable minimum coupling gap of 0.125 mm, the minimum θ_1 of the proposed phase shifter is 54°, thus $(f_2/f_1)_{\max} = (180°–54°)/54° = 2.3$. Under all circumstances, the phase shift characteristics within the dual-passband only have slightly fluctuate.

To achieve different absolute bandwidths of the two passbands, the bandstop network can be properly designed with different center frequencies. As shown in Fig. 4, when θ_c increases form 0.95 θ_0 to θ_0 and 1.05 θ_0, the bandstop network shifts to the upper band, and the ratios of the absolute bandwidths of the two passbands gradually decrease, which are derived as $(f_2\Delta_2)/(f_1\Delta_1) = 1.45$, $(f_2\Delta_2)/(f_1\Delta_1) = 1$, and $(f_2\Delta_2)/(f_1\Delta_1) = 0.68$, respectively. In addition, the center frequency ratio of the two passbands also decreases gradually. As for its phase characteristics, similarly, the phase shift response is almost unchanged no matter how the bandstop network varies.

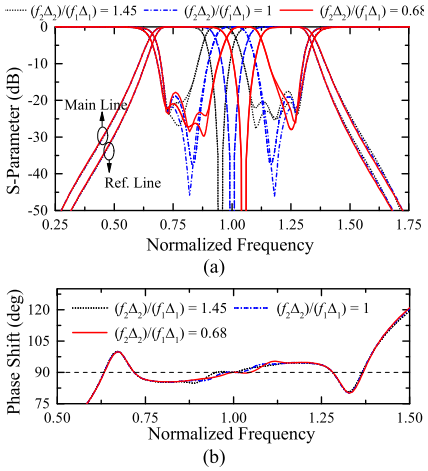

Fig. 4. Simulated responses of the proposed differential phase shifter under different center frequencies of the bandstop network ($Z_c = 50\ \Omega$, $Z_d = 150\ \Omega$). (a) Amplitude. (b) Phase shift.

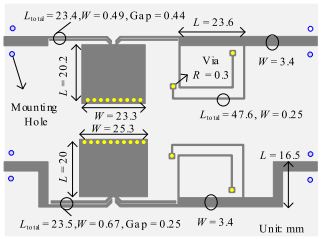

Fig. 5. Layout of the fabricated dual-band filtering differential phase shifter.

From the above analysis, it can be confirmed that the phase shift and dual-band amplitude characteristics of the proposed differential phase shifter are relatively independent, and the two passbands are capable of achieving the same phase shift values with the desired frequency ratio and absolute bandwidths.

IV. Demonstration and Results

To verify the abovementioned method, a dual-band phase shifter is designed, in which the frequency ratio is $f_2/f_1 = 2.4/1.6 = 1.5$, absolute bandwidth ratio is $(f_2\Delta_2)/(f_1\Delta_1) = 1$, and the phase shift is $90° \pm 5°$. Then $\theta_1 = 65°$, $\theta_2 = 115°$, $\theta_3 = 88°$, and $\theta_4 = 92°$ can be calculated, respectively. Finally, the initial parameters are derived as: $Z_{em} = 141.3\ \Omega$, $Z_{om} = 60.2\ \Omega$, $Z_{1m} = 9.8\ \Omega$, $Z_{er} = 162.9\ \Omega$, $Z_{or} = 75.9\ \Omega$, $Z_{1r} = 10\ \Omega$, $Z_c = 50\ \Omega$, and $Z_d = 150\ \Omega$. The used substrate is RO4003C with a dielectric constant of 3.55 and a thickness of 1.524 mm. The diagram of the fabricated circuit prototype is given in Fig. 5. Electromagnetic simulation is executed by Keysight Advanced Design System (ADS), and the measurement is done by using the vector network analyzer R&S ZNB20.

Three sets of calculated, simulated, and measured results are provided in Fig. 6. The measured center frequencies in the two passbands are 1.6 and 2.45 GHz, and the minimum in-band insertion losses are 0.5 and 0.8 dB, respectively. The measured bandwidths with return loss larger than 16 dB are 19.3% and 12%, respectively. In addition, the phase shifter achieves over 24-dB stopband suppression among 3–5 GHz. As for its phase characteristics, the measured phase shift bandwidth and phase deviation for the first band are 1.43–1.79 GHz (i.e., $FBW_{PD} = 22.5\%$) and $90° \pm 2.4°$, and that for the second passband are 2.14–2.57 GHz (i.e., $FBW_{PD} = 17.7\%$) and $90° \pm 5°$, respectively. The measured and simulated results are in good agreement, and a slight frequency offset is caused by the fabrication tolerance. Table I provides a comparison between the proposed differential phase shifter and previous works. It can be clearly exhibited that the proposed work can indeed feature independently controllable phase shift and dual passband responses, as well as the same phase shifts.

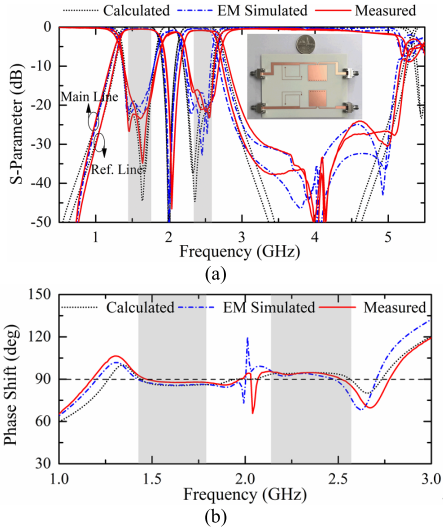

Fig. 6. Calculated, electromagnetic (EM) simulated, and measured results of the proposed differential phase shifter. (a) Amplitude. (b) Phase shift.

TABLE I
Performance Comparison With Previous Works

Ref.	Phase Shift ±PD, °	*IL* (dB)	*RL* (dB)	FBW (%)	Size* (λ_g^2)	Amp & Pha Independent	$\Delta\varphi_2 = \Delta\varphi_1$
[11]	45±2 46±2	1.1 1.2	15 15	10 10	0.04	No	No
[12]	163 59	0.12 0.12	38 38	–	0.29	No	No
[13]	45.6 -44.6	0.29 0.23	33 38	–	0.03	No	No
[14]	180±3 90±2	1.2 1.3	10 10	14 17	0.09	No	No
[15]	270±15 90 ±6.4	1.5 0.8	10 10	14 60	0.24	No	No
This work	90±5 90±2.4	1.2 0.7	16 16	12 19	0.17	Yes	Yes

IL/RL: the maximum insertion loss and the minimum return loss. λ_g: The guided wavelength at the lower-band center frequency. *: Estimated path size.

V. Conclusion

In this letter, a dual-band filtering differential phase shifter using cascaded wideband phase shifter and the bandstop network is proposed. Through theoretical analysis, it is well revealed that after cascading a bandstop network, phase shift characteristic of the phase shifter remains unchanged, while wideband filtering characteristic in amplitude is turned into dual passbands. Therefore, the proposed one features its advantage of achieving the same phase shifts within two controllable passbands. Finally, experimental results are given to validate the proposed design concept well. The proposed dual-band differential phase shifter may find its potential applications in a point-to-multipoint multibeam phased array and dual-fed CP antennas.

REFERENCES

[1] B. M. Schiffman, "A new class of broad-band microwave 90-degree phase shifters," *IEEE Trans. Microw. Theory Techn.*, vol. MTT-6, no. 2, pp. 232–237, Apr. 1958.

[2] X. Tang and K. Mouthaan, "Phase-shifter design using phase-slope alignment with grounded shunt $\lambda/4$ stubs," *IEEE Trans. Microw. Theory Techn.*, vol. 58, no. 6, pp. 1573–1583, Jun. 2010.

[3] S. Y. Zheng, W. S. Chan, and K. F. Man, "Broadband phase shifter using loaded transmission line," *IEEE Microw. Wireless Compon. Lett.*, vol. 20, no. 9, pp. 498–500, Sep. 2010.

[4] Y.-X. Guo, Z.-Y. Zhang, and L. C. Ong, "Improved wide-band Schiffman phase shifter," *IEEE Trans. Microw. Theory Techn.*, vol. 54, no. 3, pp. 1196–1200, Mar. 2006.

[5] A. M. Abbosh, "Ultra-wideband phase shifters," *IEEE Trans. Microw. Theory Techn.*, vol. 55, no. 9, pp. 1935–1941, Sep. 2007.

[6] Q. Liu, Y. Liu, J. Shen, S. Li, C. Yu, and Y. Lu, "Wideband single-layer 90° phase shifter using stepped impedance open stub and coupled-line with weak coupling," *IEEE Microw. Wireless Compon. Lett.*, vol. 24, no. 3, pp. 176–178, Mar. 2014.

[7] J. Zhou, H. J. Qian, and X. Luo, "Compact wideband phase shifter using microstrip self-coupled line and broadside-coupled microstrip/CPW for multiphase feed-network," *IEEE Microw. Wireless Compon. Lett.*, vol. 27, no. 9, pp. 791–793, Sep. 2017.

[8] X. Y. Pu, S. Y. Zheng, J. Liu, Y. Li, and Y. Long, "Novel multi-way broadband differential phase shifter with uniform reference line using coupled line structure," *IEEE Microw. Wireless Compon. Lett.*, vol. 25, no. 3, pp. 166–168, Mar. 2015.

[9] H. Zhu and Y. J. Guo, "Wideband filtering phase shifter using transversal signal-interference techniques," *IEEE Microw. Wireless Compon. Lett.*, vol. 29, no. 4, pp. 252–254, Apr. 2019.

[10] Y.-P. Lyu, L. Zhu, and C.-H. Cheng, "Proposal and synthesis design of differential phase shifters with filtering function," *IEEE Trans. Microw. Theory Techn.*, vol. 65, no. 8, pp. 2906–2917, Aug. 2017.

[11] X. Tang and K. Mouthaan, "Dual-band class III loaded-line phase shifters," in *Proc. Asia–Pacific Microw. Conf.*, Dec. 2010, pp. 1731–1734.

[12] K. Rawat and F. M. Ghannouchi, "Design methodology for dual-band Doherty power amplifier with performance enhancement using dual-band offset lines," *IEEE Trans. Ind. Electron.*, vol. 59, no. 12, pp. 4831–4842, Dec. 2012.

[13] A. M. Zaidi, S. A. Imam, B. K. Kanaujia, K. Rambabu, K. Srivastava, and M. T. Beg, "A new dual band 4×4 butler matrix with dual band 3 dB quadrature branch line coupler and dual band 45° phase shifter," *AEU-Int. J. Electron. Commun.*, vol. 99, pp. 215–225, Feb. 2019.

[14] Y.-P. Lyu, L. Zhu, and C.-H. Cheng, "Dual-band differential phase shifter using phase-slope alignment on coupled resonators," *IEEE Microw. Wireless Compon. Lett.*, vol. 28, no. 12, pp. 1092–1094, Dec. 2018.

[15] Q. Dong, Y. Wu, W. Chen, Y. Yang, and W. Wang, "Single-layer dual-band bandwidth-enhanced filtering phase shifter with two different predetermined phase-shifting values," *IEEE Trans. Circuits Syst. II, Exp. Briefs*, vol. 68, no. 1, pp. 236–240, Jan. 2021, doi: 10.1109/TCSII.2020.3008532.

[16] L.-L. Qiu and L. Zhu, "Balanced wideband phase shifters with good filtering property and common-mode suppression," *IEEE Trans. Microw. Theory Techn.*, vol. 67, no. 6, pp. 2313–2321, Jun. 2019.

[17] L.-C. Tsai and C.-W. Hsue, "Dual-band bandpass filters using equal-length coupled-serial-shunted lines and Z-transform technique," *IEEE Trans. Microw. Theory Techn.*, vol. 52, no. 4, pp. 1111–1117, Apr. 2004.

[18] J.-S. Hong and M. J. Lancaster, *Microstrip Filter for RF/Microwave Application*. New York, NY, USA: Wiley, 2001.